Journal of Colloid and Interface Science 351 (2010) 457–465

Contents lists available at ScienceDirect

Journal of Colloid and Interface Science

www.elsevier.com/locate/jcis

Adsorption and aggregation of 2-hydroxyl-propanediyl-α,ω-bis(dimethyldodecyl ammonium bromide) in aqueous solution: Effect of intermolecular hydrogen-bonding

Xiaomei Pei, Yi You, Jianxi Zhao *, Yongshu Deng, Erjun Li, Zhenxiang Li

Institute of Colloid and Interface Chemistry, College of Chemistry and Chemical Engineering, Fuzhou University, Fuzhou, Fujian 350108, PR China

ARTICLE INFO

Article history:
Received 14 May 2010
Accepted 29 July 2010
Available online 4 August 2010

Keywords:
Adsorption and aggregation
Hydroxyl substituted spacer
Intermolecular hydrogen bonding

ABSTRACT

The adsorption and aggregation of 2-hydroxyl-propanediyl-α,ω-bis(dimethyldodecyl ammonium bromide) (abbreviated as 12-3(OH)-12) in aqueous solution have been investigated by equilibrium and dynamic surface tension, surface dilational rheology, conductivity, fluorescence probing, viscosity, zeta potential and dynamic light scattering measurements. The results measured by dynamic surface tension, molar and differential conductivities strongly suggested the formation of dimolecular moieties in dilute systems prior to their adsorption and aggregation, which was attributed to intermolecular hydrogen-bonding between the hydroxyl substituted spacers. This increased the hydrophobicity of the molecular moieties and greatly promoted their adsorption at the air/water interface and association in solution. The intermolecular hydrogen-bonding between the molecules adsorbed at the air/water interface made their arrangement tighter and thus produced lower γ_{cmc} compared with unsubstituted 12-3-12. Moreover, the effect of intermolecular hydrogen bonding promotes growth of 12-3(OH)-12 micelles and leads to dissociation of the counterions on the aggregate surfaces.

1. Introduction

Compared with traditional single-headgroup and single-alkyl chain surfactants, the spacer group is a unique component part in gemini surfactant molecule, which has been known to strongly affect the self-assembly of gemini surfactants in aqueous solution [1]. So far, the various gemini surfactants containing different spacers, for example, a flexible hydrophilic [2–5], flexible hydrophobic [6,7], or rigid hydrophobic [8–11], have been investigated. Among a class of cationic gemini surfactants containing hydroxyl substituted spacer interests us [12–18]. We expect that these surfactants can produce the intermolecular hydrogen-bonding between the substituted spacers when they adsorb at air/water interface or associate in bulk solution.

Generally, the process of self-assembly of surfactant at air/water interface or in aqueous solution was attributed in large part to "hydrophobic effects" in which a major part of the driving force for forming the "organized assembly" is an entropically favored release of interfacial water [19–21]. This is a kind of nondirective driving forces and generally results in the aggregates with symmetric structure such as spherical micelles or vesicles. Different from symmetric spherical micelles and vesicles, wormlike micelle has a very long contour length ca 1 μm, which is the result of micellar growth along one-dimensional direction. Long wormlike micelles can spontaneously entangle to jelly the solution. Viscoelstical wormlike micelle solutions and supramolecular gels have extensive applications in industry [22–24]. Such systems are typically formed by adding salt to the solutions of an ionic surfactant such as cetyltrimethylammonium bromide (C_{16}TABr) [25,26]. The mechanism involved has been ascribed to the effective screening of the electrostatic repulsions between the charged head-groups, which results in a reduction of the optimal molecular area at the hydrocarbon–water interface, leading to an increase in the end-cap energy [22].

Different from hydrophobic effects, intermolecular hydrogen bonding is a directive driving force. If such a driving force could be served as the supplementary contribution to the micellar system, this will undoubtedly accelerate growth of micelles. Indeed, the role of intermolecular hydrogen bonding has been exhibited in some systems, for instance, lecithin organogel formation [27] and naphthol induced C_{16}TABr viscoelastic gel [28], etc. The gemini surfactant containing hydroxyl substituted spacer is a good candidate to investigate the contribution of intermolecular hydrogen bonding to micellar growth. Recently, we synthesized a cationic gemini surfactant 2-hydroxyl-propanediyl-α,ω-bis(dimethyldodecyl ammonium bromide) (abbreviated as 12-3(OH)-12). This gemini surfactant has one hydroxyl substituted methylene spacer compared with propanediyl-α,ω-bis(dimethyldodecyl ammonium bromide) (symbolized as 12-3-12), the latter is a gemini surfactant

* Corresponding author. Fax: +86 591 22866152.
E-mail address: jxzhao.colloid@fzu.edu.cn (J. Zhao).

0021-9797/$ - see front matter © 2010 Elsevier Inc. All rights reserved.
doi:10.1016/j.jcis.2010.07.076

studied extensively [1]. As mentioned above, the behavior of 12-3(OH)-12 in aqueous solution had been previously examined in several groups [12–18]. However, they did not focus on the role of intermolecular hydrogen bonding though the hydrogen bonds between the substituted hydroxyl group and water molecule has been suggested. In the work we are performing, 12-3(OH)-12 was found to have a greatly stronger ability of wormlike micelle-forming and to be more sensitive to the addition of salt, resulting in long wormlike micelles formed, in comparison with 12-3-12. This was perhaps due to intermolecular hydrogen bonding interaction.

If there exists the intermolecular hydrogen bonding interaction between 12-3(OH)-12 molecules, this effect also certainly affects their adsorption and association in dilute solution. In the present work we represent the results of a complementary study of 12-3(OH)-12 in aqueous dilute solution, in which the intermolecular hydrogen bonding interaction between the substituted spacers was emphatically investigated by various experimental methods. For comparison, unsubstituted 12-3-12 was also examined on the same level in order to realize the effect of the intermolecular hydrogen bonding on the adsorption and the association of 12-3(OH)-12. This will benefit us to well understand the rheological behavior of the wormlike micelle solution formed by 12-3(OH)-12.

2. Materials and methods

2.1. Materials

Gemini surfactants, 2-hydroxyl-propanediyl-α,ω-bis(dimethyldodecyl ammonium bromide) (referred below as 12-3(OH)-12) and propanediyl-α,ω-bis(dimethyldodecyl ammonium bromide) (referred to as 12-3-12), were synthesized in our laboratory according to the methods reported by Rosen [15] and Zana [7], respectively. Their chemical structures are shown in Scheme 1. All the products were confirmed by ^{1}H NMR and elemental analysis as shown in Supporting Materials.

Nile Red (NR, phenoxazone-9, Acros) that is chemically known as 9-diethylamino-5H-benzo[α]phenoxazine-5-one ($C_{20}H_{18}N_2O_2$), and 1,6-diphenylhexatriene (DPH, Fluka, HPLC grade) were used as received. Pyrene (Fluka) was re-crystallized three times in ethanol. All the solutions were prepared with Milli-Q water (resistivity = 18.2 MΩ cm^{-1}).

2.2. Measurements

2.2.1. Equilibrium surface tension

Equilibrium surface tension of the surfactant aqueous solutions was measured with CHAN DCA-315 tensionmeter equipped with a Pt–Ir du Noüy ring. The circumference of the ring is 5.930 cm. The ratio of the outside radius to the radius of the ring cross section (R/r) is 53.1218. Measurements were taken until successive values agreed to within 0.1 mN m^{-1}.

2.2.2. Dynamic surface tension

Dynamic surface tension was measured using a SINTERFACE bubble pressure tensionmeter, Model BPA-1S. The inside diameter of the capillary is 0.2 mm. The experimental uncertainties in dynamic surface tension measurements are approximately ±0.1 mN m^{-1}.

2.2.3. Surface dilational elasticity

Surface dilational elasticity measurements were carried out with an optical angle meter, OCA-20, with oscillating drop accessory ODG-20 from Dataphysics Instruments GmbH, Germany. A drop of liquid, formed from a syringe into a thermostated optical glass cuvette containing water in the bottom to avoid drop evaporation, was hung for ~ 40 min to guarantee the adsorption equilibrium. Then, the equilibrated surface was disturbed by sinusoidal oscillations. The accessible frequency range was 0.01–1 Hz and the relative area (A) variation was ~ 7%, which satisfied the requirement of linear viscoelasticity. The changes in drop shape were monitored by a CCD camera with a minimum of 50 frames per second. At the end of the experiment, the software retrieved the images and calculates the change in area and respective changes in surface tension for each cycle. Using a Fourier transform analysis, the complex dilational modulus (ε^*) and phase angle (θ) were determined and the dilational elasticity ε was calculated by

$$\varepsilon = |\varepsilon^*| \cos\theta \quad (1)$$

2.2.4. Electrical conductivity

Electrical conductivity of the sample solutions was performed using a digital conductometer (Shanghai Weiye Instrument Plant, model DDS-307 with DJS-0.1 platinum electrode. The cell constant = 0.928 cm^{-1}, provided by the manufacturer). From the experimental data, the molar conductivity Λ was determined as $(\kappa - \kappa_0)/C$, where κ_0 is specific conductivity of water. *Differential conductivity* was measured by a special conductivity cell consisted of two parts: a transfer-pipette type of conductivity cell and a round-flask type of stock bulb, and their bottoms were connected with a glass capillary. Based on the dependence of the specific conductivity, κ, on the surfactant concentration, C, the differential conductivity, $d\kappa/dC$, was defined as the increment, $(\kappa_2 - \kappa_1)/(C_2 - C_1)$ for a pair of the nearest-neighboring data [29].

2.2.5. Spherical-to-rod-to-wormlike micelle transition

Spherical-to-rod-to-wormlike micelle transition was determined by the Nile Red (NR) probing method as reported previously [30]. Fluorescence spectra of NR (2.0×10^{-6} mol L^{-1}) were recorded on a Hitachi F4500 fluorescence spectrophotometer with xenon lamp and photomultiplier detector. Slit for excitation and emission monochromators was 5.0 nm. The excitation wavelength (λ_{ex}) was 480 nm.

2.2.6. Micropolarity

Micropolarity of the aggregates was measured using steady-state fluorescence spectroscopy with pyrene as the probe [31–33]. Steady-state fluorescence emission spectra of pyrene (5×10^{-6} mol L^{-1}) were recorded by the instrument described above at λ_{ex} = 335 nm. The ratio of the emission intensity of the first to the third peaks (I_1/I_3) was used to character the polarity of the microenvironment located by pyrene that was known to solubilize in the palisade layers of the micelles [34–36].

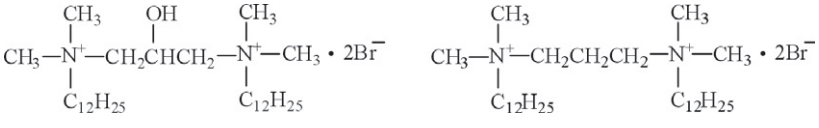

Scheme 1. Chemical structures of 12-3(OH)-12 and 12-3-12.

2.2.7. Microviscosity

Microviscosity of the aggregates was obtained by DPH probing method [33]. Fluorescence spectra of DPH were recorded on a Hitachi F4500 fluorescence spectrophotometer as described above. The excitation wavelength was 360 nm, and the emission was monitored at 435 nm. The excitation polarizer was used to measure the fluorescence anisotropy, r. The relationship between microviscosity η_i and r is

$$\eta_i = RT\tau/[V_m(r_0/r - 1)] \quad (2)$$

where R is the gas constant, T is the absolute temperature, τ is the probe lifetime in its environment, V_m is the probe effective molar volume, and r_0 is the fluorescence anisotropy in a medium of infinite viscosity. For DPH the value of r_0 is 0.362 in glycerol at −60 °C [37].

2.2.8. Zeta potential

Zeta potential measurements were performed by zeta potential analyzer (Brookhaven Instrument Corporation, USA) equipped with a microprocessor unit to measure the zeta potential. Each sample was allowed to equilibrate for 2 h under constant agitation and then kept in water-bath at 25 °C for 24 h to reach the equilibrium. The solutions were then transferred into the measurement cells for 30 min before zeta potential measurements. The final zeta potential value was taken as an average of three measurements.

2.2.9. Viscosity

Viscosity of aqueous surfactant solutions was measured with Ubbelohde viscometer. The dynamic viscosity (η) was calculated according to Eq. (3):

$$\eta = A\rho t - \frac{B\rho}{t} \quad (3)$$

where t is the efflux time, ρ is the density of sample, A and B are the calibration constants of the viscometer. When $t > 100$ s, the term of $\frac{B\rho}{t}$ can be ignored and thus the relative viscosity to the solvent water (η_r) follows Eq. (4):

$$\eta_r = \frac{\eta}{\eta_0} = \frac{t}{t_0} \quad (4)$$

where t_0 is the efflux time of solvent.

2.2.10. Rheological measurements

Rheological measurements were performed on a stress controlled rheometer (AR2000ex, TA instruments) with cone-plate sensor. The cone is made of standard ETC steel with the diameter of 20 mm and the cone angle of 2°. The gap between the center of cone and the plate is 50 μm. Each sample was kept for 5 min on the plate to reach the equilibrium before testing. A strain sweep was performed at a frequency of 6.28 rad s^{-1} (1 Hz) before the test. A strain value was then decided to make sure the sample in the linear viscoelastic region during the following oscillatory measurements.

2.2.11. Dynamic light scattering

Dynamic light scattering of micellar solutions was measured by Brookhaven Instrument which was composed of a BI-200SM goniometer, a BI-9000AT digital correlator (522 channels) and a photomultiplier detector. The He–Ne laser with 15 mW power and 632.8 nm wavelength was as the light source. All solutions were filtered through 0.22-μm Millipore filters into cylindrical light-scattering cells (od = 15 mm). The scattered light at 90° was collected and the autocorrelation function was analyzed using CONTIN software.

All the measurements were conducted at 25 °C. For light scattering measurements, the temperature was controlled by a thermostatic circulator with temperature stability ±0.01 °C (Polysceience, USA). For others a thermostat (DC-0506, Shanghai Hengping Instrument Factory) with the accuracy of ±0.1 °C was used.

3. Results and discussion

3.1. Adsorption at the air/water interface

Fig. 1 shows the equilibrium surface tension (γ) plots of 12-3(OH)-12 and 12-3-12 in aqueous solution, where the γ of 12-3(OH)-12 starts to drop at a lower concentration C than that of 12-3-12. This yields a smaller critical micelle concentration (*cmc*), indicating the stronger micelle-forming ability of 12-3(OH)-12. Moreover, 12-3(OH)-12 has a lower γ_{cmc} (33.4 mN m^{-1} at 25 °C) at the saturated adsorption in comparison with that (34.6 mN m^{-1} at 25 °C) of 12-3-12. This corresponds to a smaller area (0.54 nm^2) of 12-3(OH)-12 molecule adsorbed at the air/water interface than that (0.60 nm^2) of 12-3-12, which are calculated by Gibbs formula (Eqs. (5) and (6)) in terms of the slope ($d\gamma/d \log C$) of the dropping curve at the *cmc*. This indicates that adsorbed 12-3(OH)-12 molecules are arranged more tightly.

$$\Gamma_{\max} = -\frac{1}{2.303nRT}\frac{d\gamma}{d\log C} \quad (5)$$

where n is 2 for the salt-free system [38,39].

$$A_{\min} = \frac{1}{N_A\Gamma_{\max}} \quad (6)$$

where N_A is Avogardo constant.

Fig. 2 shows the experimental measurements of interface elasticity (ε) as a function of frequency (v) in both systems at a concentration of 0.8 times of each *cmc*. The 12-3(OH)-12 system shows greatly larger value of interface elasticity in comparison with the 12-3-12 system, demonstrating that the adsorption film of 12-3(OH)-12 is denser. This is consistent with the results obtained from the surface tension measurements.

Since 12-3(OH)-12 only differs from 12-3-12 in molecular structure with a substituted hydroxyl group in the spacer, the different adsorption phenomena are believed to come from the effect of this substituted hydroxyl group. A possible reason is formation of the hydrogen-bonding between the spacers of the adsorbed 12-3(OH)-12 molecules. The ability of hydrogen bond-forming of 12-3(OH)-12 with water has been suggested by Wettig et al. [18], however, they did not focus on the intermolecular hydrogen bonds. If so, the 12-3(OH)-12 molecules are certainly

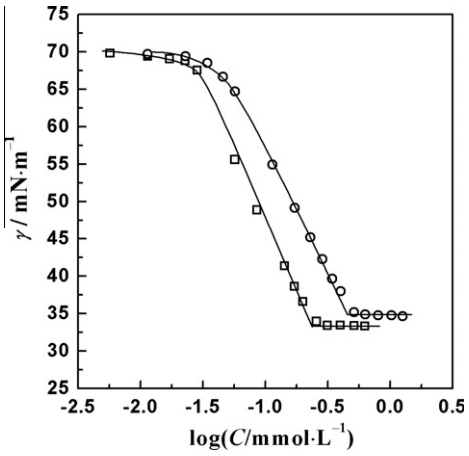

Fig. 1. Surface tension (γ) vs. log C plots for 12-3(OH)-12 (□) and 12-3-12 (○) in aqueous solution.

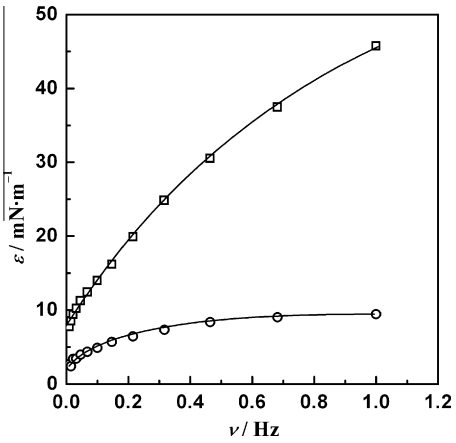

Fig. 2. Interfacial dilational elasticity (ε) vs. oscillation frequency (ν) for 12-3(OH)-12 (□) and 12-3-12 (○) in aqueous solution, where the relative concentration of the surfactant (C/cmc) is fixed at 0.8.

pulled closer, which makes the arrangement of the molecules tighter.

3.2. The state of 12-3(OH)-12 molecule in the dilute solution

Fig. 3a shows the variation of surface tension γ with time t (the plots of dynamic surface tension) at a concentration of 0.8 times of each *cmc*. The decrease of γ with increasing t is more significant for 12-3-12, whereas the γ of 12-3(OH)-12 has only a very small decrease over the range of initial time and then drops with further increasing t. According to Ward and Tordai model [40] that describes the diffusion-only controlled adsorption process, the variation of γ with t over the range of short time follows the formula:

$$\gamma_t = \gamma_0 - 2nRTC_0\sqrt{Dt/\pi} \tag{7}$$

where γ_0 is the surface tension of the solvent, C_0 is the concentration of surfactant in bulk solution and n is 2 as suggested by Li et al. [38] and Zana [39]. From the straight line slope in the plots of γ vs. $t^{1/2}$ (Fig. 3b), the diffusion coefficient Ds. of 12-3(OH)-12 and 12-3-12 can be obtained, which are $0.28 \pm 0.04 \times 10^{-11}$ and $1.05 \pm 0.16 \times 10^{-11}$ m^2 s^{-1}, respectively. As compared with 12-3-12, the far smaller D of 12-3(OH)-12 corresponds to the slower diffusion of the molecular moiety towards the interface. A reasonable explanation is the formation of oligo-aggregate ions in the 12-3(OH)-12 solution, which leads to large molecular weight of the moiety. Since this slow diffusion does not occur in the 12-3-12 system, the formation of oligo-aggregate ions must relate to intermolecular hydrogen-bonding between the substituted spacers of 12-3(OH)-12. This fact indicates that the interaction between the 12-3(OH)-12 molecules has already occurred even in dilute solution before they start to adsorb at the interface.

The evidence also comes from the results of conductivity measurements. Fig. 4a illustrates molar conductivity vs. surfactant concentration plots, in which the 12-3(OH)-12 system shows a maximum, whereas the 12-3-12 system does not. This maximum is the signature of premicellar association in surfactant solution [39,41]. It arises because the equivalent conductivity of a small aggregate of surfactant ions (dimeric or trimeric, etc.) is larger than the sum of the equivalent conductivities of the ions constituting it [41,42]. Differential conductivity technique also sensitively responds to the oligo-aggregate ions in the aqueous solution [43]. Fig. 4b gives out the comparison between the differential conductivity curves of the both at 25 °C, from which an obvious "peak" in the curve of 12-3(OH)-12 can be observed. This has been attributed to the characteristic of the oligo-aggregate ions in solution [43]. A possible dimolecular structure of 12-3(OH)-12 linked by the hydrogen bonds is schematically represented in Fig. 5, although the details of the molecules arrangement may be complicated. This mechanism reasonably explains the results shown in Figs. 1 and 2.

3.3. Micellar growth with increasing concentration

12-3-12 has a very small *cmc* compared with the corresponding monomer dodecyltrimethylammonium bromide (C_{12}TABr). This makes the micelle formed initially very small and the aggregation number was estimated to be ~ 22 [44]. With increasing the concentration, more molecules participate in the construction of micelles, resulting in rapid growth of the micelles and finally forming wormlike micelles [44]. As discussed in above sections, 12-3(OH)-12 has a stronger association ability than 12-3-12 and therefore we believe it also goes through similar process. In a very recent issue, we reported a new and sensitive fluorescence method to determine the transition of micelles from spherical-to-rod-to-wormlike using Nile Red (NR) as the probe [30], in which the I_a/I_b of NR (the fluorescence intensity ratio of the twisted intramolecular charge transfer band to the planar locally excited band) was used as the index to represent the micellar transition. Fig. 6 shows

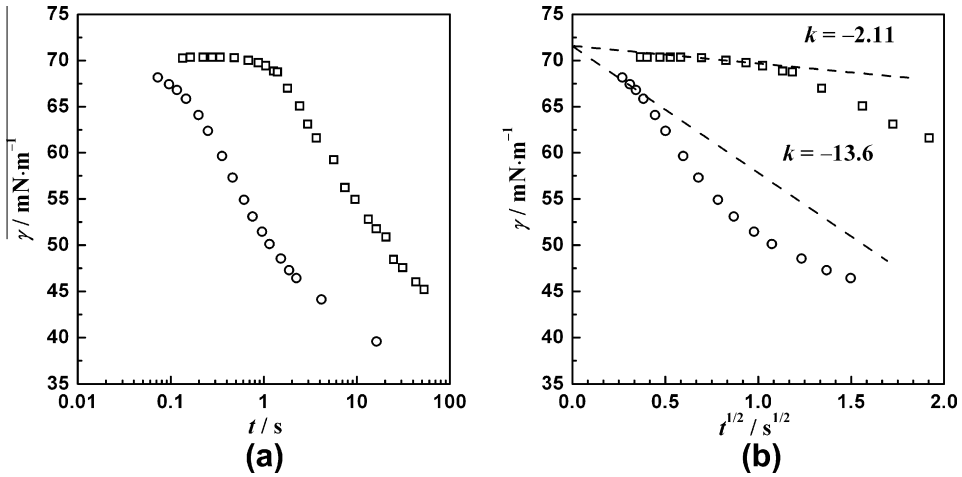

Fig. 3. (a) Surface tension (γ) vs. time (t) plots for 12-3(OH)-12 (□) and 12-3-12 (○) in aqueous solution with a concentration of 0.8 *cmc*. (b) Plots of γ against $t^{1/2}$, which derived from the original data in (a).

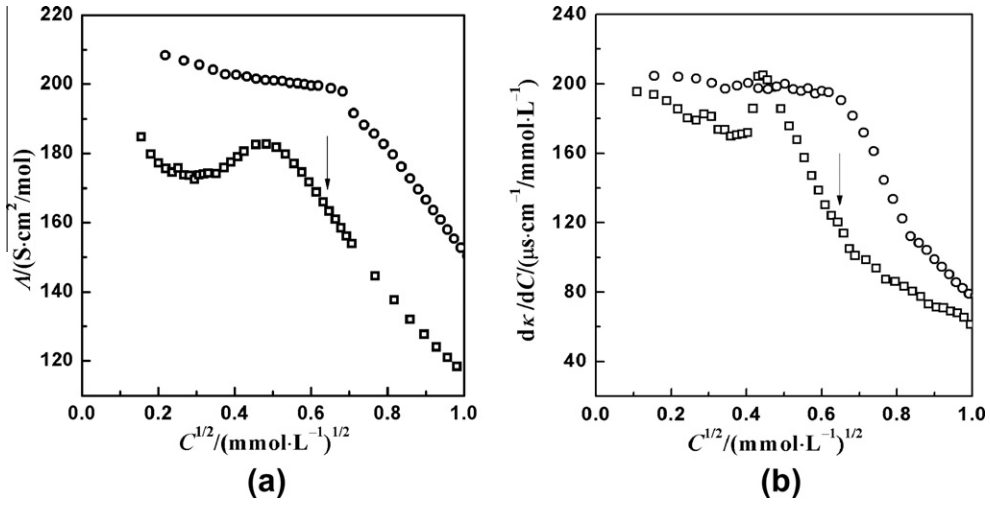

Fig. 4. Molar conductivity (Λ, *a*) and differential conductivity ($d\kappa/dC$, *b*) vs. concentration ($C^{1/2}$) plots for 12-3(OH)-12 (□) and 12-3-12 (○) in aqueous solution. The arrow indicates the *cmc* for 12-3(OH)-12 system.

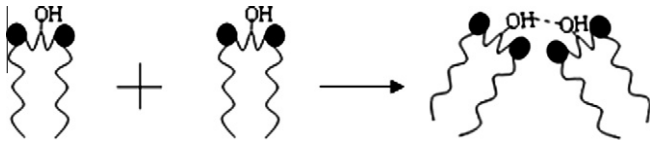

Fig. 5. A schematic representation of dimolecular structure of 12-3(OH)-12 in dilute solution.

the variation of I_a/I_b of NR with *C* for both systems, where the curves show a minimum at relatively low concentration (14.3 mmol L^{-1} for 12-3(OH)-12 and 21.1 mmol L^{-1} for 12-3-12) and then rapidly rises to a plateau. As revealed in the previous work, the minimum in the plot of I_a/I_b of NR vs. *C* indexes the critical point of the spherical-to-rod transition of micelles, whereas the point where the curve levels off corresponds to the critical one of the rod-to-wormlike transition of micelles [30]. From the comparison between the plots in Fig. 6a and b, one can see that the 12-3(OH)-12 micelles grow more rapidly than 12-3-12 ones with increasing concentration. The corresponding viscosity of the solution is well consistent with the micellar transition observation as seen in Fig. 6.

Fig. 7 shows the results of rheological measurements at the concentration of about two folds of each second critical point. The shear thinning phenomena shown in Fig. 7a and the clear viscoelastic spectra (Fig. 7b) well verify the formation of the wormlike micelles in both systems [45].

3.4. Micropolarity and microviscosity of the aggregate

In this section, we examine the micropolarity and the microviscosity of the aggregate over the region of spherical-to-rod transition. It is well known that the pyrene (Py) is a sensitive probe to determine the polarity of the microenvironment where Py is located. For this purpose the ratio of the first to the third peaks (I_1/I_3) in the Py emission spectrum was used as the index [31–33]. Over this region, 12-3(OH)-12 system shows obviously lower value of I_1/I_3 (1.28 ± 0.01) compared with that (1.40 ± 0.01) of 12-3-12. This means that the aggregates constructed by 12-3(OH)-12 has a denser structure, agreeing with the assumption of the formation of intermolecular hydrogen bonding in this system.

The microviscosity measurements also give out the similar information. In this work, the aggregate microviscosity was determined using the fluorescence probing method based on the measurement of the fluorescence anisotropy of micelle-solubilized DPH (1,6-diphenylhexatriene) [33,46]. According to Eq. (2), the variation of the product of the microviscosity, η_i, and the effective

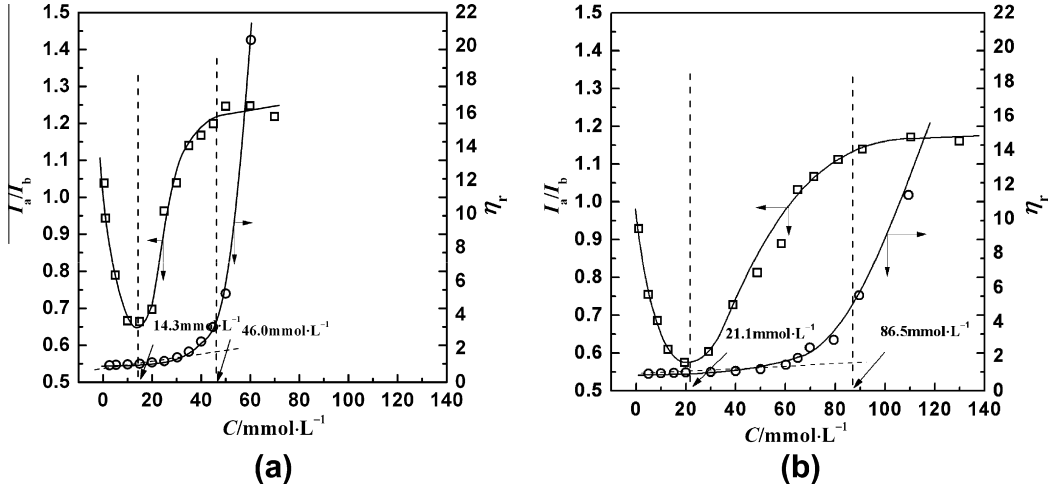

Fig. 6. Variation of I_a/I_b of NR and relative viscosity (η_r) vs. surfactant concentration (*C*) for 12-3(OH)-12 (a) and 12-3-12 (b) in aqueous solution.

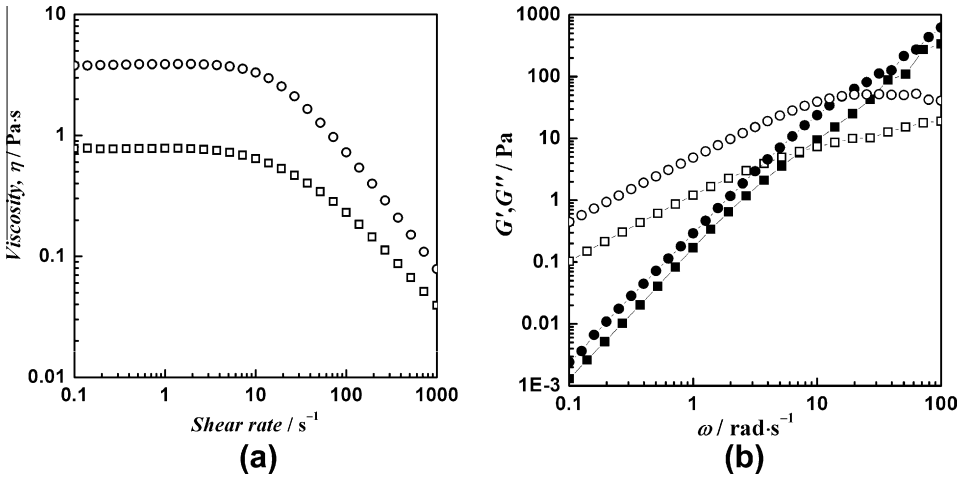

Fig. 7. Solution viscosity vs. steady shear rate curves (a) and viscoelastic spectra (b, G' (filled symbols) and G'' (open symbols)) for 12-3(OH)-12 (rectangles, 80 mmol L^{-1}) and 12-3-12 (circles, 150 mmol L^{-1}) aqueous solutions.

molar volume of DPH, V_m, with the concentration is shown in Fig. 8. At a comparable concentration, the $\eta_i V_m$ of 12-3(OH)-12 is much larger than that of 12-3-12, which is consistent with the denser structure of 12-3(OH)-12 aggregates.

3.5. Surface charge of the aggregates

Generally, the plot of specific conductivity κ vs. surfactant concentration C (Fig. 9) can be used to estimate the ionization degree of micelle (α) by the ratio of the slopes of the two straight lines above and below *cmc* (S_2 and S_1), i.e., $\alpha = S_2/S_1$ [47]. By this method, the αs of 12-3(OH)-12 and 12-3-12 are 0.24 ± 0.02 and 0.22 ± 0.02, respectively. Very close α of both was also observed by Wettig et al. [18]. Besides chemical nature of ionic headgroup, the ionization degree generally relates to the area of ionic headgroup occupied at the micellar surface [48]. The gemini micelle formed initially only has very small aggregation number [1,44] and thereby the core–shell structure of micelle may be uncompleted. That is to say, the apparent area per headgroup under this state may lose its meaning.

As mentioned in Section 1, the wormlike micelles formed by 12-3(OH)-12 were found to have a more sensitive response to the addition of electrolyte than that of 12-3-12. To understand this point, we measured the electrophoresis of the aggregates in aqueous solution over the region of rod-micelles. Fig. 10 shows the zeta potential obtained from the micellar electrophoretic mobility measurements as a function of surfactant concentration. At a comparable concentration, the zeta potential of 12-3(OH)-12 micelles

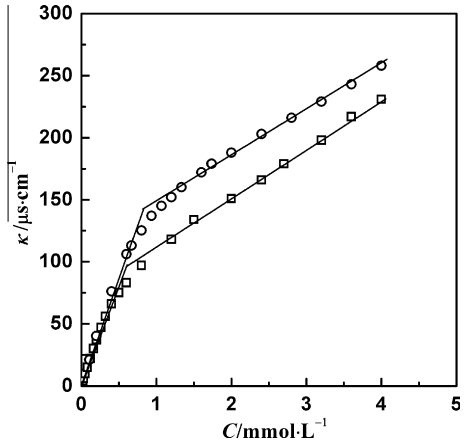

Fig. 9. Specific conductivity (κ) vs. surfactant concentration (C) for 12-3(OH)-12 (□) and 12-3-12 (○) in aqueous solution.

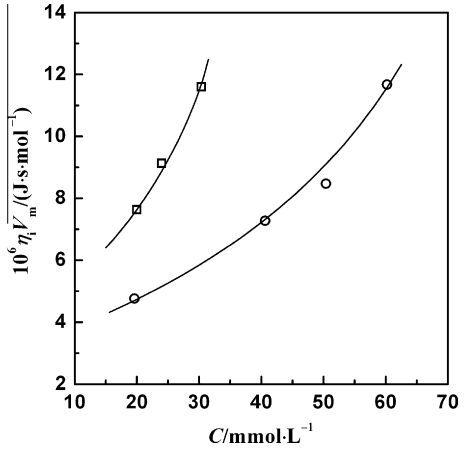

Fig. 8. Relative microviscosity ($\eta_i V_m$) vs. surfactant concentration (C) for 12-3(OH)-12 (□) and 12-3-12 (○) in aqueous solution.

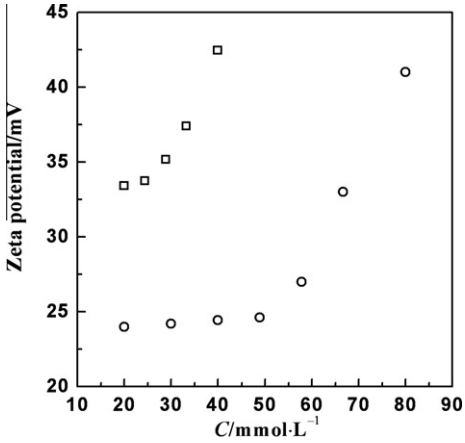

Fig. 10. Zeta potential vs. surfactant concentration (C) for 12-3(OH)-12 (□) and 12-3-12 (○) in aqueous solution.

is greatly larger than that of 12-3-12. The micelle size over this range was examined by dynamic light scattering technique. Fig. 11 shows the normalized electric field autocorrelation functions of 12-3(OH)-12 at 40 mmol L^{-1} and 12-3-12 at 40 and 80 mmol L^{-1}, respectively, which were represented as $\beta|g^{(1)}(\tau)|^2$ according to the Siegert relation [49]:

$$g^{(2)}(\tau) = 1 + \beta|g^{(1)}(\tau)|^2 \quad (8)$$

where $g^{(2)}(\tau)$ is normalized intensity autocorrelation function that can be experimentally measured, β is a non-ideality factor accounting for the deviation from the ideal correlation and τ is the delay time. The electric field autocorrelation functions are excellently fitted by the CONTIN model as shown by the solid lines and thus the CONTIN model is used to analyze the light scattering data. Fig. 12 illustrates the intensity–fraction distribution for the three samples, from which the mean effective hydration diameters of the micelles are obtained to be 30.4 nm for 12-3(OH)-12 at 40 mmol L^{-1}, 24.7 nm and 29.5 nm for 12-3-12 at 40 and 80 mmol L^{-1}, respectively. At the same concentration of 40 mmol L^{-1}, the micelle of 12-3(OH)-12 has a larger size than that of 12-3-12, well reflecting the accelerated growth of the former due to the role of the intermolecular hydrogen bonding. The relative variance of 12-3(OH)-12 is only 0.004, indicating the micelles are very monodisperse. Contrarily, both systems of 12-3-12 show large relative variance, which are 1.839 and 1.633, respectively, meaning polydispersity of the micelle size. This situation is certainly relevant to the intermolecular hydrogen bonding, which strengthens the intermolecular interactions and promotes the formation of the tightly packed structure. In a word, at a comparable concentration, the 12-3(OH)-12 micelle has a larger size and a denser structure in comparison with the 12-3-12 micelle. This undoubtedly leads to more charges on the surface of 12-3(OH)-12 micelle in comparison with 12-3-12 micelle. On the other hand, the intermolecular hydrogen bonding also induces the increase in the hydrophilicity on the aggregate surfaces, which is favorable to the release of the counterions. All the factors make 12-3(OH)-12 micelles larger zeta potential and more sensitive to respond the addition of electrolyte than 12-3-12 micelles.

Let us return to Fig. 9 to explain lower specific conductivity of 12-3(OH)-12 at micelle region than 12-3-12 using the results of dynamic light scattering. This situation is consistent with the observation of Wettig et al. [18], in which they also found substituted 12-4(OH)-12 and 12-4$(OH)_2$-12 had lower specific conductivity than unsubstituted 12-4-12 but did not discuss it. Obviously, 12-3(OH)-12 micelle with a large size moves slowly than 12-3-12 micelle. This may be the reason producing relatively low conductivity in 12-3(OH)-12 system.

4. Summary

A comparative study has been conducted in solutions of cationic gemini surfactants 12-3(OH)-12 that contains a hydroxyl substituted spacer and unsubstituted 12-3-12. The results clearly show that the intermolecular hydrogen bonds are formed between the

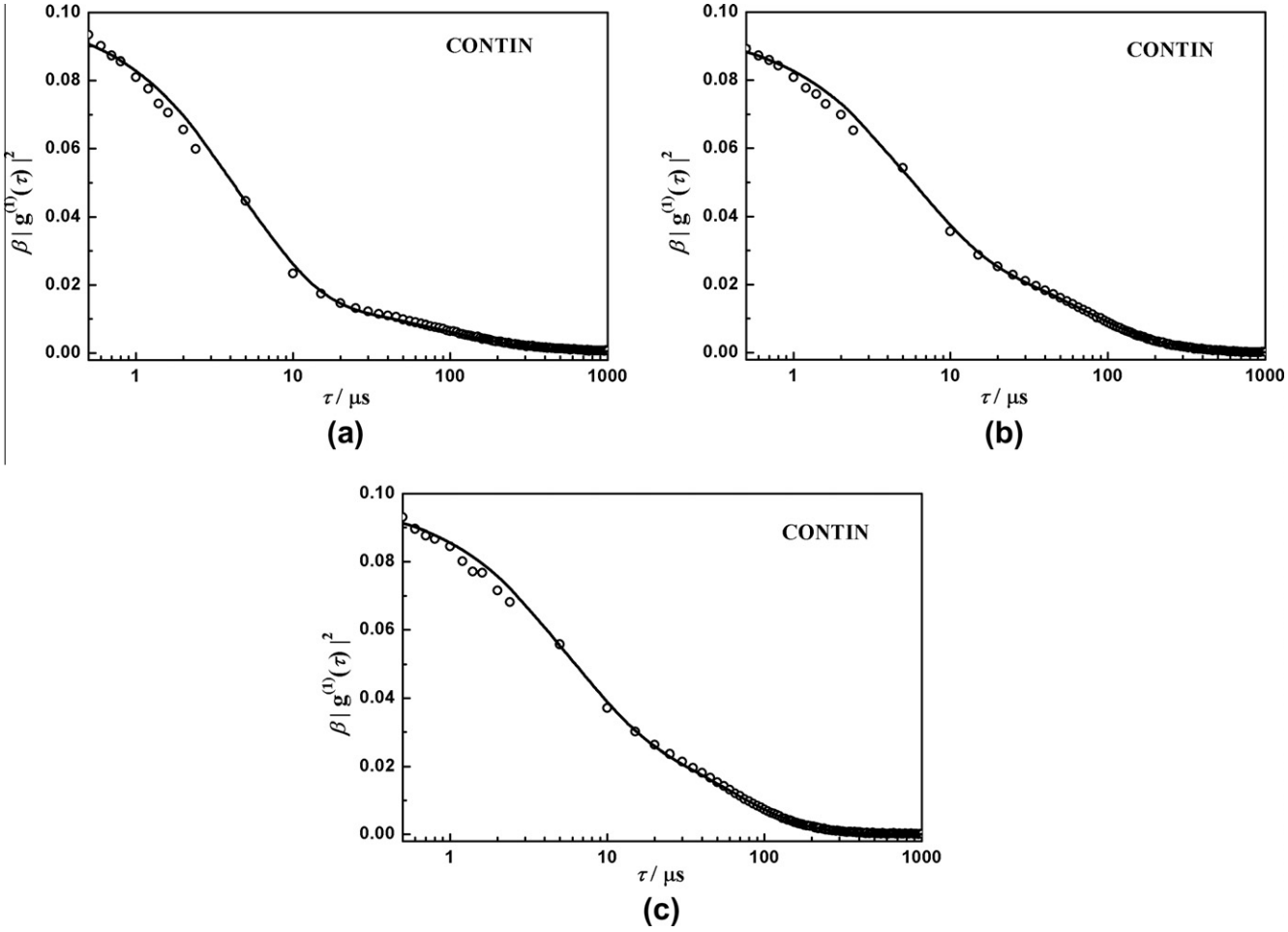

Fig. 11. The normalized electric field autocorrelation functions of 12-3(OH)-12 solution at 40 mmol L^{-1} (a), 12-3-12 solutions at 40 mmol L^{-1} (b) and at 80 mmol L^{-1} (c). The solid lines are the fitted results by the CONTIN model.

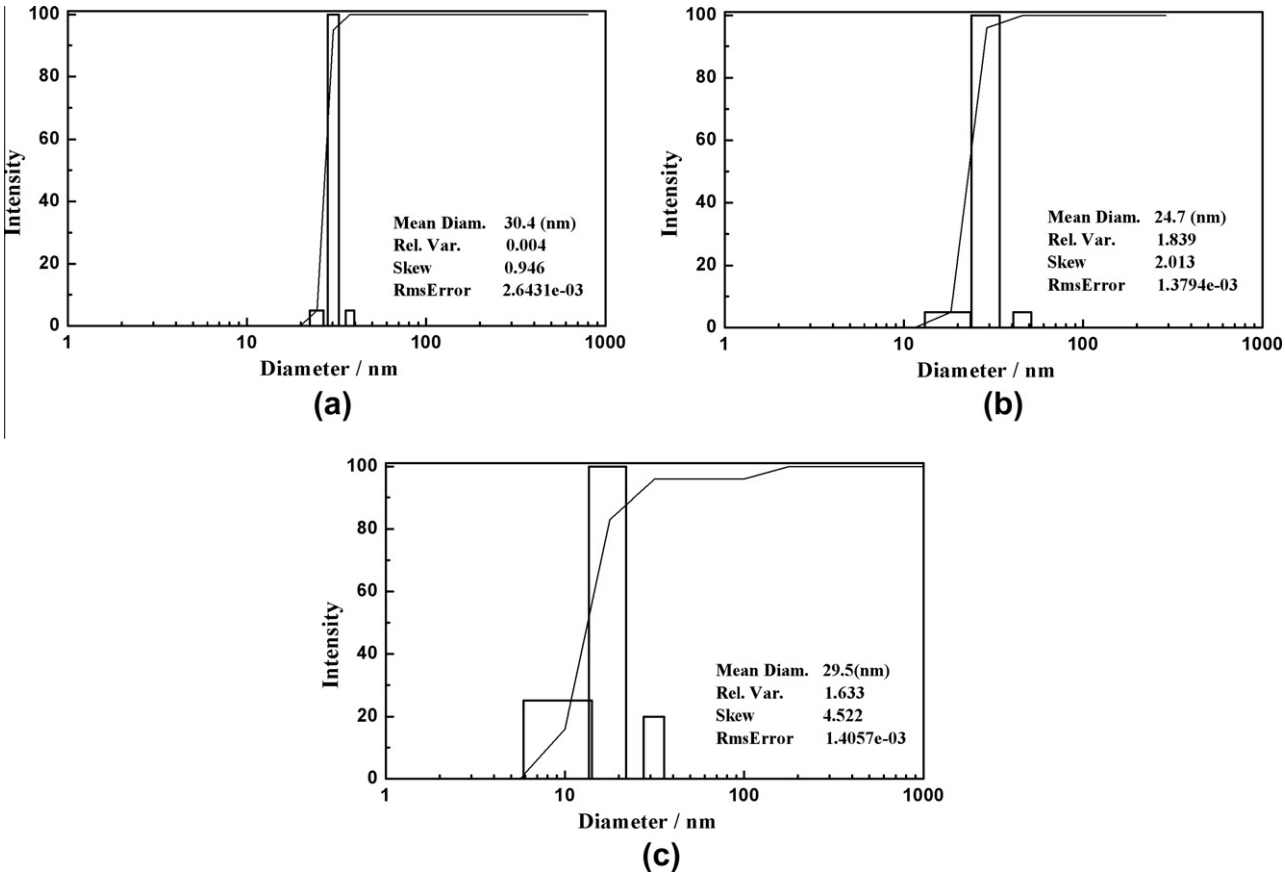

Fig. 12. Intensity-fraction distribution for 12-3(OH)-12 solution at 40 mmol L^{-1} (a), 12-3-12 solutions at 40 mmol L^{-1} (b) and at 80 mmol L^{-1} (c).

substituted 12-3(OH)-12 molecules, which leads to the dimer formation even in dilute solution before they start to adsorb at the interface. This results in stronger adsorption and association of 12-3(OH)-12 in comparison with unsubstituted 12-3-12. Obviously, the effect of the intermolecular hydrogen bonding also remains in the organized assembly such as the adsorption film and the aggregates and thus strongly affects their properties. Different from generally hydrophobic effects, intermolecular hydrogen bonding is a directive driving force. When this effect is served as the supplementary contribution to the micellar system, it is favorable to accelerate growth of micelles. The present results suggest that a simple hydroxyl substitution in the spacer of gemini surfactant can achieve the goal of effectively utilizing the effect of intermolecular hydrogen bonding in the construction of the aggregates with more complicated structure such as wormlike micelles. By this point of view, the gemini surfactants with hydroxyl substituted spacer may be good candidates to construct viscoelastic wormlike micellar systems. This subject will be further discussed in detail in the following issue.

Acknowledgment

Support from the National Natural Science Foundation of China (20673021 and 20873024) is gratefully acknowledged.

Appendix A. Supplementary material

Supplementary data associated with this article can be found, in the online version, at doi:10.1016/j.jcis.2010.07.076.

References

[1] R. Zana, J. Xia, Gemini Surfactants: Synthesis Interfacial and Solution-Phase Behavior and Applications, Marcel Dekker, New York, 2004.
[2] M. Okahara, A. Masuyama, Y. Sumida, Y.P. Zhu, J. Jpn. Oil Chem. Soc. 37 (1988) 716.
[3] Y.P. Zhu, A. Masuyama, M. Okahara, J. Am. Oil Chem. Soc. 68 (1991) 268.
[4] M.J. Rosen, Z.H. Zhu, X.Y. Hua, J. Am. Oil Chem. Soc. 69 (1992) 30.
[5] A. Masuyama, T. Hirono, Y.P. Zhu, M. Okahara, M.J. Rosen, J. Jpn. Oil Chem. Soc. 41 (1992) 301.
[6] F. Devinsky, I. Lacko, F. Bittererova, L. Tomeckova, J. Colloid Interface Sci. 114 (1986) 314.
[7] R. Zana, M. Benrraou, R. Rueff, Langmuir 7 (1991) 1072.
[8] F.M. Menger, C.A. Littau, J. Am. Chem. Soc. 113 (1991) 1451.
[9] F.M. Menger, C.A. Littau, J. Am. Chem. Soc. 115 (1993) 10083.
[10] B.L. Song, Y.F. Hu, Y.M. Song, J.X. Zhao, J. Colloid Interface Sci. 341 (2010) 94.
[11] R. Jiang, Y.H. Ma, J.X. Zhao, J. Colloid Interface Sci. 297 (2006) 412.
[12] M.J. Rosen, L. Liu, J. Am. Oil Chem. Soc. 73 (1996) 885.
[13] T.S. Kim, T. Kida, Y. Nakatsuji, T. Hirao, I. Ikeda, J. Am. Oil Chem. Soc. 73 (1996) 907.
[14] L.D. Song, M.J. Rosen, Langmuir 12 (1996) 1149.
[15] M.J. Rosen, L.D. Song, J. Colloid Interface Sci. 179 (1996) 261.
[16] M.J. Rosen, J.H. Mathias, L. Davenport, Langmuir 15 (1999) 7340.
[17] J.H. Mathias, M.J. Rosen, L. Davenport, Langmuir 17 (2001) 6148.
[18] S.D. Wettig, P. Nowak, R.E. Verrall, Langmuir 18 (2002) 5354.
[19] C. Tanford, The Hydrophobic Effects: Formation of Micelles and Biological Membranes, Wiley, New York, 1980.
[20] R. Nagarajan, E. Ruckenstein, Langmuir 7 (1991) 2934.
[21] F.M. Menger, Micelles, Microemulsions and Monolayers, Marcel Dekker, New York, 1998.
[22] C.A. Dreiss, Soft Matter 3 (2007) 956.
[23] S. Ezrahi, E. Tuval, A. Aserin, Adv. Colloid Interface Sci. 77 (2006) 128. and references therein.
[24] K. Trickett, J. Eastoe, Adv. Colloid Interface Sci. 144 (2008) 66. and references therein.
[25] A. Khatory, F. Lequeux, F. Kern, S.J. Candau, Langmuir 9 (1993) 1456.
[26] T. Shikata, H. Hirata, T. Kotaka, Langmuir 3 (1987) 1081.
[27] Y.A. Shchipunov, Colloids Surf., A 183–185 (2001) 541.
[28] S.K. Saha, M.J. Moazzam, A.A. Chakraborty, G. Bit, S.K. Das, J. Phys. Chem. B 112 (2008) 4642.

[29] M. Manabe, M. Funamoto, F. Kohgami, H. Kawamura, H. Katsuura, Colloid Polym. Sci. 281 (2003) 239.
[30] C.Y. Lin, J.X. Zhao, Dyes Pigm. 84 (2010) 223.
[31] K. Kalyansundaram, J.K. Thomas, J. Am. Chem. Soc. 99 (1977) 2039.
[32] D.C. Dong, M.A. Winnik, Can. J. Chem. 62 (1984) 2560.
[33] R. Zana, M. In, H. Lévy, G. Duportail, Langmuir 13 (1997) 5552.
[34] O. Zheng, J.X. Zhao, J. Colloid Interface Sci. 300 (2006) 749.
[35] P. Mukerjee, J.R. Cardlnal, J. Phys. Chem. 82 (1978) 1620.
[36] B. Valeur, Molecular Fluorescence, Principles and Applications, Wiley-VCH, New York, 2001.
[37] M. Shinitzky, I. Yuli, Chem. Phys. Lipids 30 (1982) 261.
[38] Z.X. Li, C.C. Dong, R.K. Thomas, Langmuir 15 (1999) 4392.
[39] R. Zana, J. Colloid Interface Sci. 248 (2002) 203.
[40] V.D. Fainerman, A.V. Makievski, R. Miller, Colloids Surf., A 87 (1994) 61.
[41] R. Zana, J. Colloid Interface Sci. 246 (2002) 182.
[42] A. Pinazo, X. Wen, L. Pérez, M.R. Infante, Langmuir 15 (1999) 3134.
[43] M. Manabe, The differential conductivity technique and its application to mixed surfactant solutions for determining ionic constants, in: Mixed Surfactant Systems, Marcel Dekker, New York, 2005.
[44] D. Danino, Y. Talmon, R. Zana, Langmuir 11 (1999) 1448.
[45] R.G. Shrestha, L.K. Shrestha, K. Aramaki, J. Colloid Interface Sci. 311 (2007) 276.
[46] R. Zana, Surfactant Solutions, New Methods of Investigation, Marcel Dekker, New York, 1987.
[47] H. Hirata, N. Hattori, M. Ishida, H. Okabayashi, M. Frusaka, R. Zana, J. Phys. Chem. 99 (1995) 17778.
[48] R. Zana, J. Colloid Interface Sci. 78 (1980) 330.
[49] B. Chu, Laser Light Scattering: Basic Principles and Practice, second ed., Academic Press, Boston, 1974 (Chapter 3).